Martensitic microstructure and its damping behavior in $Ni_{52}Mn_{16}Fe_8Ga_{24}$ single crystals

W. H. Wang* and X. Ren

Materials Physics Group, National Institute for Materials Science, 1-2-1 Sengen, Tsukuba 305-0047, Japan

G. H. Wu

*Beijing National Laboratory for Condensed Matter Physics, Institute of Physics, Chinese Academy of Science, Beijing 100080,
People's Republic of China*

In the present study, the martensitic microstructure and its damping behavior in $Ni_{52}Mn_{16}Fe_8Ga_{24}$ single crystals were investigated using differential scanning calorimetry (DSC), x-ray diffraction (XRD), transmission electron microscopy (TEM), and dynamical mechanical analyzer (DMA). A structural transition from the cubic austenite to orthorhombic seven-layered modulation martensite was confirmed by XRD experiments and TEM observations. The measurements of temperature dependence of internal friction (IF) reveal an additional very broad IF peak in the low-temperature martensite phase. Moreover, the IF peak is frequency independent but it shows a pronounced amplitude dependence behavior, i.e., the IF peak broadens, decreases in height, and shifts to lower temperature with the increase of amplitude. The related mechanisms are also discussed in terms of the martensitic microstructure.

Ferromagnetic shape memory alloys (FSMAs) are expected as a key ingredient in future high performance actuating devices. Therefore, in recent years, many FSMAs, such as Ni-Mn-Ga,[1] Co-Ni-Ga,[2,3] Fe-Pd,[4] and Fe-Pt,[5] have been developed. Among them, Ni-Mn-Ga is the mostly studied alloy, and there have been many reports on its structure, magnetic properties, martensitic transformation, magnetically controlled shape memory effect, and magnetic-field-induced strains (MFIS).[6–20] So far, it has been generally accepted that MFIS is due to the magnetically induced movement of martensitic twin boundaries which, at the same time, are magnetic domain walls. The stoichiometric alloy of Ni_2MnGa shows the highest Curie temperature of ~376 K, the largest saturated magnetization of 100 emu/g in martensite at 4 K, largest magnetic moment per formula of 4.17 μ_B, but a quite low martensitic transformation temperature of ~202 K.[6] In order to increase the transformation temperature to room temperature for the device application, the composition of the compound was usually modified from the stoichiometry. But, their output stress becomes smaller partly due to the smaller saturation magnetization, and the operating range is also limited by relatively low Curie temperatures (320–360 K).[12,13] Therefore, many groups are actively searching new magnetic shape memory alloys with a larger magnetization and a higher Curie temperature.[14–16]

Recently, we have reported a giant magnetic-field-enhanced MFIS in a Fe-doped $Ni_{52}Mn_{16}Fe_8Ga_{24}$ single crystal.[19] Further studies on the influence of the Fe content on the martensitic transformations and magnetic properties revealed that the existence of Fe in Ni-Mn-Ga alloys caused a stronger magnetic exchange interaction leading to higher Curie temperatures.[20] These results imply that the Fe-doped quaternary alloys are especially promising from the point of view of applications. However, despite the findings of the previous works, a careful structural analysis, especially the evolution of microstructure associate with the martensitic transformation is still lacking. It is well known that most of

the properties of FSMAs are strongly dependent not only on the composition, but also on the microstructure of the alloys. More recently, Ni-Mn-Ga-polymer composites have been found to show strong vibration damping behavior due to the motion of martensite variants.[21] This means that the damping behavior of shape memory materials is highly sensitive to their microstructure. However, the damping behavior of martensite in a Fe-doped Ni-Mn-Ga system so far is not reported to the best of our knowledge. In this paper, we will present a systematical study of martensitic microstructure and its damping behavior in $Ni_{52}Mn_{16}Fe_8Ga_{24}$ single crystals.

The single crystals of $Ni_{52}Mn_{16}Fe_8Ga_{24}$ were grown by the Czochralski method. The growth process and characterization of the magnetic properties and magnetic shape memory effect were described in detail elsewhere.[19] Specimens of appropriate sizes were spark cut from the initial rods and polished to obtain flat surfaces. Differential scanning calorimetry (DSC) was used to determine the martensitic transformation temperatures (see Fig. 1). The martensitic transformation temperature Ms, and the reverse transformation temperature As, and the Curie temperature Tc are 275,
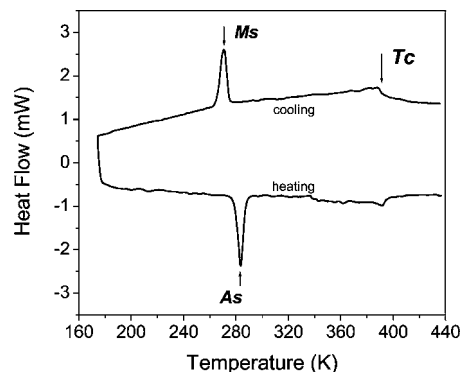

FIG. 1. DSC measurement during cooling and heating for a piece of single crystal $Ni_{52}Mn_{16}Fe_8Ga_{24}$.
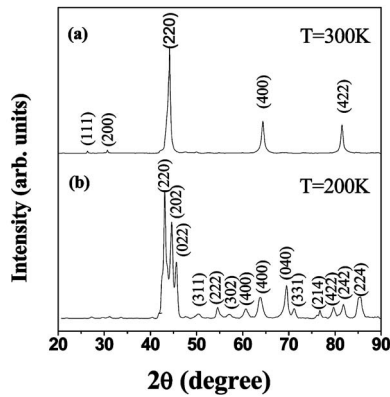
FIG. 2. Powder XRD patterns of the single crystal $Ni_{52}Mn_{16}Fe_8Ga_{24}$ measured at 300 K (a), indexed according to the cubic ($L2_1$) structure; and at 200 K (b), indexed according to the orthorhombic structure.

285, and 385 K, respectively. These results are in good agreement with our previous measurements of magnetization, resistivity, and strain.[19,20] The structural changes and phase identification of martensites were performed by means of x-ray diffraction (XRD) diffractometer equipped with cooling and heating sample stages. Thin-foil specimens for transmission electron microscope (TEM) observations were prepared by twin-jet electropolishing using an electrolyte consisting of 20 vol % HNO_3-80 vol % CH_3OH. TEM observations were performed by the JEOL 2000FX TEM (200 KV) equipped with a double-tilt cooling and heating sample stages. Additionally, the internal friction [denoted by internal friction (IF)] measurements were performed on a dynamic mechanical analyzer (DMA, Q800 from TA Instruments) in infrasonic frequency range. The sample for the DMA measurements was oriented by x-ray scattering and it was cut as a parallelepiped (12 mm × 2 mm × 1 mm in size) with the large face parallel to the {110} planes. The DMA measurements were performed in a single cantilever mode by applying a small ac bending stress perpendicular to the {110} planes.

Figure 2 shows the powder XRD pattern for the $Ni_{52}Mn_{16}Fe_8Ga_{24}$ single crystal after being crushed into fine powder at different temperatures. As shown in Fig. 2(a), at room temperature, all XRD peaks can be indexed by a cubic structure with lattice parameters of $a=b=c=5.790$ Å, and $\alpha=\beta=\gamma=90°$, which exhibits that our $Ni_{52}Mn_{16}Fe_8Ga_{24}$ single crystals are single phase and compositionally homogeneous. Moreover, the (111) superlattice reflection corresponding to the next-nearest-neighbor $L2_1$ ordering is also observed. This is in agreement with a structural criterion for Heusler alloy as was used in the case of Ni_2MnGa.[6] As the temperature is lowered to 200 K, as shown in Fig. 2(b), some new peaks, such as (302) and (214), emerged. The original $(220)_{cubic}$ peak splits into three peaks, i.e., $(220)_{orth}$, $(202)_{orth}$, and $(022)_{orth}$. The $(400)_{cubic}$ and $(422)_{cubic}$ peaks also have similar splitting behavior. To index these characteristic peaks, we confirmed that the martensitic transformation in our $Ni_{52}Mn_{16}Fe_8Ga_{24}$ sample is from the cubic ($L2_1$ ordering) to an orthorhombic structural transition. The orthorhom-
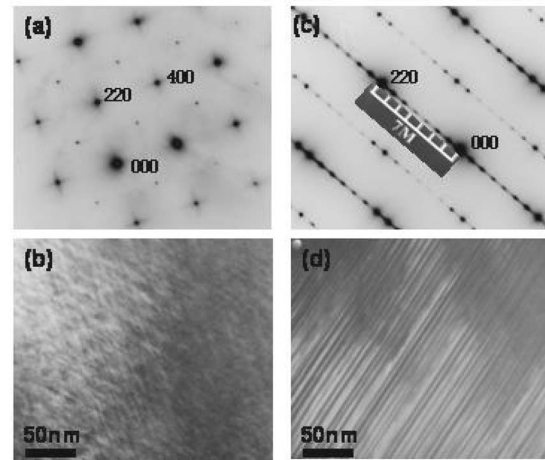

FIG. 3. (a) Electron-diffraction pattern taken at room temperature along the $[001]_p$ zone axis direction, exhibiting the additional reflection spots. (b) The corresponding TEM image observed at room temperature. (c) Electron-diffraction pattern taken at low temperature of 200 K along $[001]_p$ zone axis, showing the presence of superstructures along $\langle 110 \rangle_p$ orientation. (d) The corresponding TEM image showing the 7M superstructures.

bic phase has lattice parameters: $a=6.081$ Å, $b=5.833$ Å, $c=5.507$ Å, and $\alpha=\beta=\gamma=90°$.

To microscopically characterize the features of the structural transition, *in situ* TEM observations were performed on our single crystal $Ni_{52}Mn_{16}Fe_8Ga_{24}$ sample, by varying the temperature from room temperature to 200 K. Figures 3(a) and 3(b) show the selected area electron diffraction pattern (SAEDP) and the corresponding TEM bright image observed at room temperature. In the parent phase (denoted by p), the diffraction pattern can be well indexed by a cubic $L2_1$ structure with lattice parameter of $a=5.780$ Å, which is in good agreement with the value calculated from the XRD pattern. In addition, the observed rodlike diffuse scattering of the fundamental reflections along the $\langle 110 \rangle_p$ directions and the characteristic "tweed" contrast observed in the TEM bright field image [Fig. 3(b)], have been interpreted in terms of a pretransitional softening of the [110]-TA_2 phonon branch along $\langle 110 \rangle_p$ directions in Heusler alloys.[9,22] Upon cooling, the diffuse reflections progressively sharpened and the modulation periodicity increased gradually and then finally turned out to be discontinuous superstructure spots at Ms (275 K). Figure 3(c) shows a typical superstructure appearing in the basic crystal plane taken in the low-temperature martensite phase of 200 K. (To find the lattice correspondence between the high-temperature parent phase and the low-temperature martensite phase, the latter one is also indexed by the $L2_1$ lattice.) We can clearly see that this superstructure appears along the $\langle 110 \rangle_p$ directions with a wavelength of seven times the distance between $\{220\}_p$ planes, i.e., the unit reciprocal lattice distance along the $\langle 110 \rangle_p$ directions is divided into seven equal parts by six extra spots marked by arrows. Conventionally, it is called seven-layered modulation (7M) martensite. In Fig. 3(d), we show the corresponding TEM image illustrating this kind of 7M superstructures in an area.
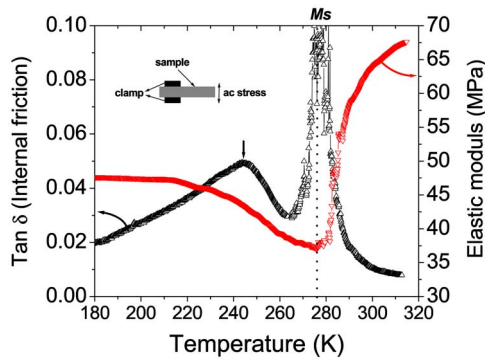
FIG. 4. (Color online) Temperature dependence of elastic modulus and internal friction during cooling between 300 and 180 K for single crystal $Ni_{52}Mn_{16}Fe_8Ga_{24}$. The measurement was performed at a frequency of 1 Hz, and a constant amplitude of ~ 2 μm. An additional very broad IF peak appears at temperatures about 30 K below the martensitic transformation temperature Ms. The inset shows the schematic of configuration of the single cantilever clamp with sample loaded.

Figure 4 shows the typical temperature dependence of elastic modulus and internal friction during cooling between 300 and 180 K for single crystal $Ni_{52}Mn_{16}Fe_8Ga_{24}$. The measurement was performed at a frequency of 1 Hz, and a constant stress amplitude of ~ 2 μm. As expected, the internal friction curve gives rise to a large peak at Ms, where the associated elastic modulus exhibits a dip. Moreover, from Fig. 4, we can find two noticeable "characteristic" differences from that of undoped Ni-Mn-Ga single crystals. First, both in the parent and the 7M martensite phases, the values of elastic modulus are much higher than that of undoped Ni-Mn-Ga single crystals.[9] Here, we should emphasize that the very poor mechanical property, in particular the high brittleness of Ni-Mn-Ga alloys, is one of biggest challenges faced in advancing this material toward applications. The present work suggests that this poor mechanical property, probably, can be improved through doping new elements into ternary alloys of the type Ni-Mn-Ga. Second, and most remarkably, an additional very broad IF peak appears at temperatures roughly 30 K below Ms, as marked by the arrow. By contrast, the temperature dependence of elastic modulus does not exhibit any abnormal trace in this temperature regime. It can be therefore concluded that no other phase transition occurs after the 7M martensite is formed.

For a better understanding of the origin of the IF peak in low-temperature martensite phase, the frequency dependence of the internal friction measurements are helpful. In Fig. 5(a), we show the temperature dependence of internal friction during cooling at various frequencies (0.1–100 Hz) for single crystal $Ni_{52}Mn_{16}Fe_8Ga_{24}$. It can be seen that the IF peak exhibits a frequency independence behavior, i.e., the position of the IF peak does not shift with increasing frequency and, correspondingly, the height of the IF peak remains practically constant. For comparison, we have also measured the stress-amplitude dependence of the internal friction for single crystal $Ni_{52}Mn_{16}Fe_8Ga_{24}$ and the results are shown in Fig. 5(b). Interestingly, we found that the IF peak shows a pronounced stress-amplitude dependence be-
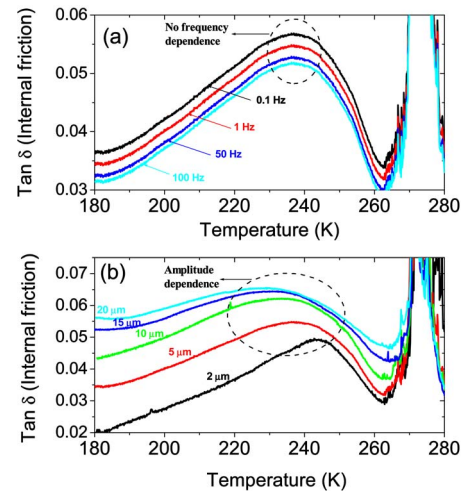

FIG. 5. (Color online) (a) Temperature dependence of internal friction (IF) during cooling at various frequencies (0.1–100 Hz) and a constant amplitude of ~ 5 μm. (b) Temperature dependence of internal friction (IF) during cooling at various amplitudes (2–20 μm) and a constant frequency of 1 Hz.

havior, that is, the IF peak broadens, decreases in height, and shifts to lower temperature with increasing stress amplitude.

The question arises as to the reason for the appearance of the IF peak at low-temperature martensite phase. In fact, being symmetry lowering and first order in nature, in the transformed martensite state, the microstructure of Ni-Mn-Ga Heusler alloys consist of different ferroelastic domains (or martensite twins) of the same structure and energy, but of different orientations with respect to each other across the {110} planes.[6] The ferroelastic domains self-organized spontaneously in the low-temperature martensite state to minimize transformation free energy. Therefore, one likely mechanism for the IF peak in the low-temperature martensite state is related to the movement of ferroelastic domains. To the best of our knowledge, however, the movement process of the ferroelastic domains is thermally activated and therefore, is normally frequency dependent (for example, in conventional NiTi-based shape memory alloys).[23] Interestingly, this important feature, being characteristic of the movement of ferroelastic domains, is absent in our $Ni_{52}Mn_{16}Fe_8Ga_{24}$ single crystals, which does not exhibit frequency dependence of the IF-peak temperature. On the contrary, our experimental results indicate that the position of the IF peak in low-temperature phase is stress-amplitude dependent, and shifts to lower temperatures with increasing stress amplitude.

On the other hand, in comparison with conventional shape memory alloys, a rather unique feature of ferromagnetic shape memory alloys is that the magnetic domains are considered to be magnetoelastically coupled to and superimposed upon ferroelastic domains that are formed upon undergoing the martensitic transformation. Due to the magnetoelastic coupling between the ferroelastic and magnetic domains, the free energy minimization during the self-organization of ferroelastic domains requires a reconfiguration of the magnetic domains when the geometry of the ferroelastic domains is altered by an applied stress. (Con-

versely, a change in magnetic domains configuration by application of magnetic field should reconfigure the ferroelastc domains). A direct evidence of this magnetoelastic coupling between magnetic domains and ferroelastic domains has recently been shown by H. D. Chopra *et al.* in an undoped Ni-Mn-Ga single crystal using the high-resolution interference-contrast-colloid (ICC) technique.[24] Therefore, we proposed that the origin of the IF peak and its amplitude dependence behavior is considered to result from a mutual accommodation of ferroelastic twin domains in order to conform to an externally applied strain. Detailed studies are currently in progress, which are aimed at establishing a quantitative correlation between the internal friction behavior and microscopic readjustment of ferroelastic and magnetic domains in our $Ni_{52}Mn_{16}Fe_8Ga_{24}$ single crystal.

In summary, by means of DSC, XRD, TEM, and DMA measurements, we have investigated the martensitic microstructure and its damping behavior in $Ni_{52}Mn_{16}Fe_8Ga_{24}$ single crystals. A structural transition from cubic $L2_1$ austenite to orthorhombic 7M martensite was confirmed by XRD experiments and TEM observations. The measurements of temperature and frequency dependence of internal friction (IF) reveal an additional IF peak in the low-temperature martensite phase. The position of the IF peak is stress-frequency independent but it shows a stress amplitude dependent behavior. The peak decreases with increasing stress amplitude, thus pointing to an intrinsic origin. Nevertheless, the reason for its origin is not yet understood and needs further study.

*Present address: Nanotechnology Research Institute, National Institute of Advanced Industrial Science and Technology (AIST), 1-1-1 Umezono, Tsukuba 305-8568, Japan. Electronic address: wang.wenhong@aist.go.jp

[1] K. Ullakko, J. K. Huang, C. Kantner, R. C. O'Handley, and V. V. Kokorin, Appl. Phys. Lett. **69**, 1966 (1996).

[2] M. Wuttig, J. Li, and C. Craciunescu, Scr. Mater. **44**(10), 2393 (2001).

[3] Y. X. Li, H. Y. Liu, F. B. Meng, L. Q. Yan, G. D. Liu, X. F. Dai, M. Zhang, Z. H. Liu, J. L. Chen, and G. H. Wu, Appl. Phys. Lett. **84**, 3594 (2004).

[4] N. W. Hagood, H. Kimura, and T. Watanabe, Mater. Trans., JIM **39**, 1248 (1998).

[5] T. Kakeshita, T. Takeuchi, T. Fukuda, M. Tsujiguchi, T. Saburi, R. Oshima, and S. Muto, Appl. Phys. Lett. **77**, 1502 (2000).

[6] P. J. Webster, K. R. A. Ziebeck, S. L. Town, and M. S. Peak, Philos. Mag. B **49**, 295 (1984).

[7] R. D. James and M. Wuttig, Philos. Mag. A **77**, 1273 (1998).

[8] R. C. O'Handley, J. Appl. Phys. **83**, 3263 (1998).

[9] V. A. Chernenko, C. Segui, E. Cesari, J. Pons, and V. V. Kokorin, Phys. Rev. B **57**, 2659 (1998).

[10] G. H. Wu, C. H. Yu, L. Q. Meng, J. L. Chen, F. M. Yang, S. R. Qi, W. S. Zhan, Z. Wang, Y. F. Zheng, and L. C. Zhao, Appl. Phys. Lett. **75**, 2990 (1999).

[11] R. Tickle, R. D. James, T. Shield, M. Wuttig, and V. V. Kokorin, IEEE Trans. Magn. **35**(5), 4301 (1999).

[12] Yanwei Ma, S. Awaji, K. Watanabe, M. Matsumoto, and N. Kobayashi, Solid State Commun. **113**, 671 (2000).

[13] V. V. Khovailo, T. Takagi, A. N. Vasilev, H. Miki, M. Matsumoto, and R. Kainuma, Phys. Status Solidi A **183**, R1 (2001).

[14] F. Zuo, X. Su, P. Zhang, G. C. Alexandrakis, F. Yang, and K. H. Wu, J. Phys.: Condens. Matter **13**, 2607 (2001).

[15] W. H. Wang, G. H. Wu, J. L. Chen, W. S. Zhan, Z. Wang, Y. F. Zheng, and L. C. Zhao, Appl. Phys. Lett. **77**, 3245 (2000).

[16] W. H. Wang, G. H. Wu, J. L. Chen, S. X. Gao, W. S. Zhan, G. H. Wen, and X. X. Zhang, Appl. Phys. Lett. **79**, 1148 (2001).

[17] W. H. Wang, Z. H. Liu, J. Zhang, J. L. Chen, G. H. Wu, W. S. Zhan, T. S. Chin, G. H. Wen, and X. X. Zhang, Phys. Rev. B **66**, 052411 (2002).

[18] A. Sozinov, A. A. Likhachev, N. Lanska, and K. Ullakko, Appl. Phys. Lett. **80**, 1746 (2002).

[19] G. H. Wu, W. H. Wang, J. L. Chen, L. Ao, Z. H. Liu, W. S. Zhan, T. Liang, and H. B. Xu, Appl. Phys. Lett. **80**, 634 (2002).

[20] Z. H. Liu, M. Zhang, W. Q. Wang, W. H. Wang, J. L. Chen, G. H. Wu, F. B. Meng, H. Y. Liu, B. D. Liu, J. P. Qu, and Y. X. Li, J. Appl. Phys. **92**, 5006 (2002).

[21] J. Feuchtwanger, S. Michael, J. Goldie, d. Bono, J. K. Huang, R. C. O'Handley, S. M. Allen, and A. Beerkowitz, J. Appl. Phys. **93**, 8528 (2003).

[22] J. Q. Li, Z. H. Liu, H. C. Yu, M. Zhang, Y. Q. Zhou, and G. H. Wu, Solid State Commun. **126**, 323 (2003).

[23] See, for example, K. Otsuka and X. Ren, Prog. Mater. Sci. **50**, 511 (2005).

[24] H. D. Chopra, C. Ji, and V. V. Kokorin, Phys. Rev. B **61**, R14913 (2000).